Available online at www.sciencedirect.com
ScienceDirect
Journal of Sound and Vibration 304 (2007) 831–844
JOURNAL OF SOUND AND VIBRATION
www.elsevier.com/locate/jsvi

Detecting weak sinusoidal signals embedded in a non-stationary random broadband noise—A simulation study

W.L. Lee[a], S.K. Tang[a,*], C.M. Chan[b]

[a]*Department of Building Services Engineering, The Hong Kong Polytechnic University, Hong Kong, China*
[b]*The Hong Kong Community College, Hong Kong, China*

Received 19 January 2007; received in revised form 6 March 2007; accepted 18 March 2007
Available online 2 May 2007

Abstract

In the present study, a simple numerical function is proposed for use together with the time–frequency analysis in the detection of very weak sinusoidal signals embedded in a non-stationary random broadband background noise. Its performance is studied through the use of two numerical examples. It is found that the present method enables good recovery of the sinusoidal signals and the instants of their initiations even when the signal-to-noise ratio is down to −17 dB.

1. Introduction

Signal detection technique has wide applications in both physics and engineering (for instance, Refs. [1,2]). For a modernized heavily serviced building, the early detection of fault signals from rotary machineries, such as the chillers, pumps, motors, etc., is crucial to its smooth operation [3]. Similar situation appears in electricity power plants. The magnitudes of the fault signals are usually very small when the faults are in their initial stages. Though the faults will usually result in abnormal spectral peaks in the machine vibration signals [4], their detection is not straightforward in the initial stage because of the presence of much stronger background signals or noises, which can be stationary or non-stationary.

Owing to the importance of signal detection in the machine health monitoring/diagnosis process, many analysis approaches have been introduced in the past few decades. The short-time Fourier transform (STFT) [5] appears to be a very obvious choice. The use of the Wigner distribution and wavelet transforms for analyzing non-stationary signals has also been studied [6,7]. Tang [8] investigated the performance of STFT and the harmonic wavelets [9] in retrieving parameters of exponential decaying pulses. Besides, the use of time series techniques for signal analysis has been examined. For example, Zhan and Jardine [10] analyzed gear faults using the auto-regression, while Chan et al. [11] investigated decaying sinusoidal pulses using the stochastic volatility approach. However, though there has been much effort made in improving signal detection and analysis, many of the proposed approaches fail to give satisfactory results when the signal-to-noise ratio (S/N) is close to 0 dB or goes negative, which is the case in the early development of a fault in the

*Corresponding author. Tel.: +852 27667782; fax: +852 27746146.
E-mail address: besktang@polyu.edu.hk (S.K. Tang).

0022-460X/$ - see front matter © 2007 Elsevier Ltd. All rights reserved.
doi:10.1016/j.jsv.2007.03.024

building services equipment. Li and Qu [12] investigated the use of the chaotic oscillator for weak signal detection, but their method requires knowledge on the characteristics of the signals to be detected.

The focus of the present study is on enhancing the detection of weak signals embedded in a stronger non-stationary signal/noise. A numerical treatment to the original signal made up of the weak sinusoidal signal and the non-stationary noise, which can facilitate a better retrieval of the weak signal after the time–frequency procedure, is proposed. Its performance is examined through two illustrative examples.

2. Theoretical considerations

The target of the present study is to establish a method to detect effectively a sinusoidal signal under a poor S/N. This section describes the development of the method. The spectral technique will be used, but it is believed that the method also works for wavelet transforms. In the foregoing analysis, all parameters are non-dimensional. Also, Ω denotes random noise with vanishing mean and magnitude bounded between ± 1 in the foregoing discussions. These signals are generated using the software MATLAB.

It is understood that the extraction of a very weak sinusoidal signal from a background noise consists of many different frequency components is difficult. One needs a method to down-weigh the effect of the background noise in the spectral calculation. A method which tends to reduce the magnitudes of the time series data but preserves the periodicity of the sinusoidal signal will be very useful. It is expected a pulse-like train will be created if one can preserve the peaks and troughs of the sinusoidal signal while the other parts of the signal are down-weighted together with the noise in the very ideal case.

2.1. Power spectral density of a square pulse train

An infinite square pulse train is perhaps the most fundamental signal in building services engineering other than the sinusoidal wave. It is given by the expression

$$x(t) = A \sum_{i=-\infty}^{\infty} (-1)^i [U(t - it_o - (t_o - \Delta)/2) - U(t - it_o - (t_o + \Delta)/2)], \tag{1}$$

where U is the unit step function, and A and Δ are real constants which fix the magnitude and duration of each pulse in $x(t)$, respectively. The period is $2t_o$. Fig. 1 illustrates an example of the train with $A = 1$, $t_o = 10$ and $\Delta = 6$. The power spectral density of x, $P(x, \omega)$, is [13]

$$P(x, \omega) = \lim_{T \to \infty} \frac{2}{T^2} \left| \int_0^T x(t) e^{-j\omega t} \, dt \right|^2, \tag{2}$$

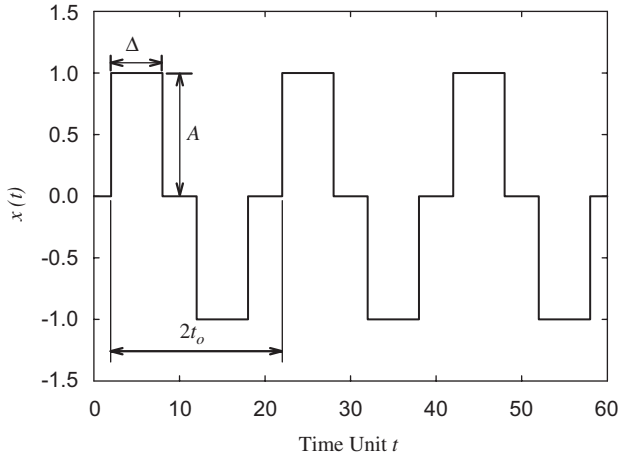

Fig. 1. Example of a square pulse train and the nomenclatures. $\Delta = 6$, $A = 1$, $t_o = 10$.

where $j = \sqrt{-1}$ and ω the angular frequency. Suppose n pulses exist within the period T, then one can approximate that for very large T and n, $T \sim nt_o$ and

$$P(x,\omega) = \frac{8}{(nt_o)^2}\left[\frac{A}{\omega}\sin\left(\frac{\omega\Delta}{2}\right)\right]^2\left|\sum_{i=0}^{n-1}(-1)^i e^{-j\omega t_o(i+0.5)}\right|^2. \tag{3}$$

For $n \to \infty$, P is only significant when $\omega = \pi/t_o$ and

$$P(x,\pi/t_o) = \frac{8A^2}{\pi^2}\sin^2\left(\frac{\pi\Delta}{2t_o}\right). \tag{4}$$

If the amplitude of each pulse in the train is not constant, but is uniformly distributed between 0 and A, the average amplitude will be $A/2$ and P will be reduced by 4 times. It can therefore be concluded that the detection of a sinusoidal wave in the presence of a random background noise will be enhanced if a numerical procedure that can transform the wave into a pulse-like train of the appropriate width can be found as the spectral contents of the random frequency components will be attenuated more quickly than that of the sinusoidal wave after the transformation. However, this may not be true if the relative size of the effective Δ with respect to the signal period is too small after the transformation.

2.2. The transformation function and its properties

A function which is simple enough for quick numerical application is required. In order to transform the sinusoidal wave into a pulse-like train, the crests and troughs of the wave must be preserved while the regions of large gradient must be down weighted to small values together with the background noise as discussed in the beginning of Section 2. The function must also be an odd function. The following function:

$$w(x) = 2x^{(2\alpha+1)}/(1+x^{2\beta}), \tag{5}$$

where α and β are non-zero integers appear to fit the present purpose. Subsequent transformations are hereinafter denoted by $w^{(1)} = w(x)$, $w^{(2)} = w(w(x))$, $w^{(3)} = w(w(w(x)))$ and so on. Fig. 2 illustrates the $w^{(1)}$ of the cosine wave $x(t) = \cos(0.02\pi t)$ for various α with $\beta = 1$. One can notice that the effective Δ is reduced after repeated transformation, but the increase in the Δ reduction is much less pronounced for large α. Increasing β at a fixed α tends to flatten slightly the crests and troughs of the transformed wave (not shown here). This is in fact true for other combinations of α and β. Repeated transformation using the same combination of α and β results in more rapid reduction of the pulse width than that produced by increasing α. Such effect at $w^{(3)}$ for $\alpha = \beta = 1$ is already stronger than that obtained by increasing α from 1 to 4 at β fixed at unity

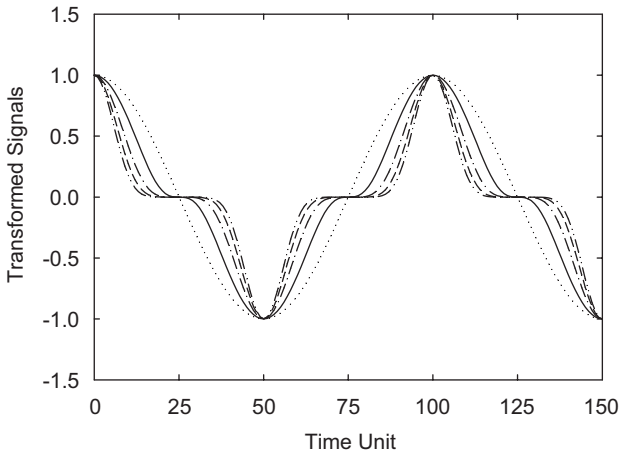

Fig. 2. Examples of transformed cosine waves with $\beta = 1$. ⋯⋯: Original wave $\cos(0.02\pi t)$; ——: $\alpha = 1$; — · —: $\alpha = 2$; — —: $\alpha = 3$; — · · —: $\alpha = 4$.

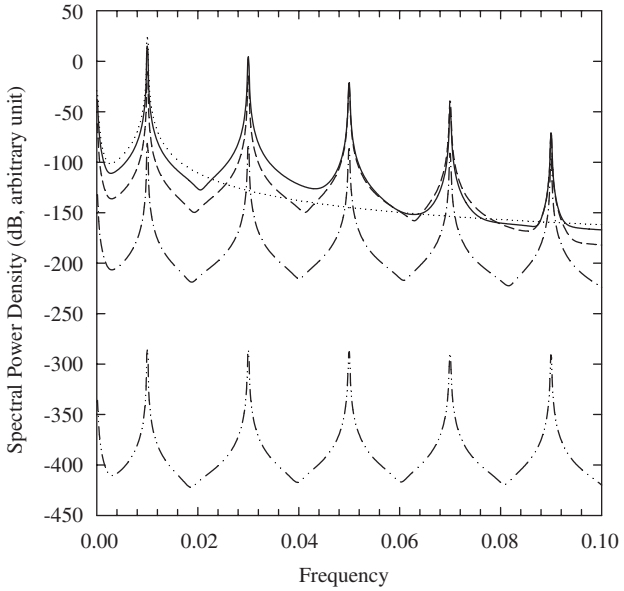

Fig. 3. Spectral power densities of transformed cosine wave $x(t) = 0.5\cos(0.02\pi t)$; ⋯⋯ : x; —— : $w^{(1)}$;— · —: $w^{(2)}$;— —: $w^{(3)}$;— · · —: $w^{(4)}$. $\alpha = \beta = 1$.

(not shown here). It should be noted that for sinusoidal wave of amplitude less than unity, each transformation will also result in a reduction of the pulse amplitude.

Fig. 3 shows the associated power spectral densities of the transformed cosine wave $x(t) = 0.5\cos(0.02\pi t)$ for $\alpha = \beta = 1$. It is noted that harmonics appear after the transformation of the cosine wave. The first three transformation using w results in faster attenuation of the average spectral energy levels of the random noise $0.5\,\Omega$ compared to the peak spectral energy of the cosine wave as shown in Fig. 4, which is expected from the deduction discussed in the previous section. Since the width of the pulse is reduced after each transformation, repeated transformation will eventually smooth out the spectral signatures of all discrete frequency components as suggested by Eq. (4). This leads to the higher spectral attenuation of $x(t) = 0.5\cos(0.02\pi t)$ after the fourth transformation. Similar phenomenon is expected to happen for the wave with unity amplitude after the fifth or the sixth transformation. One can also observe that the first two transformations tend to attenuate more the spectral power density of the random noise for smaller magnitude signals. Since the ratio of the spectral power density is around 4000 for the untransformed case, it can be concluded that the detection of the sinusoidal wave may still be possible if its amplitude is ~2% of that of the random noise without any transformation, but the isolation of its spectral peak will be extremely difficult because of the very spurious spectral peaks resulted from the random noise.

Fig. 5a and b illustrates the $w^{(4)}$s of the wave $x(t) = 0.5\cos(0.02\pi t)$ and $0.5\,\Omega$, respectively. The very periodical structure of the transformed cosine wave compared to that of the transformed random noise should enable a better detection of the wave in the presence of the random noise using the spectral method, even though the attenuation of the random noise is less serious compared to that of the cosine wave after this fourth transformation. This will be discussed further in the next section. It is also observed that there are more negative spikes than positive ones in Fig. 5b. The numbers of these spikes depend on Ω and there are other Ωs that produce more positive spikes (not shown here).

3. Illustrative examples and discussion

In this section, the effectiveness of the function w in resolving weak signals embedded inside a broadband random noise is illustrated. Two signals will be examined. The first one is a weak but steady sinusoidal signal and the other one is an abruptly generated sinusoidal signal that grows exponentially with time.

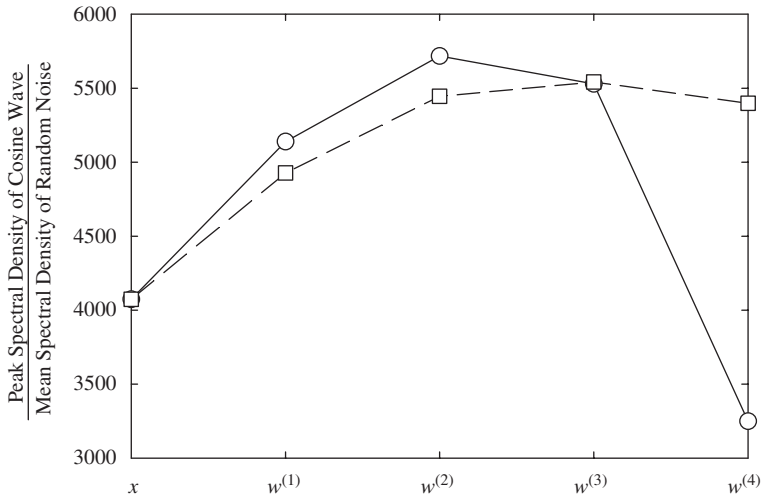

Fig. 4. Spectral power density attenuations due to repeated transformations. ○: $\cos(0.02\pi t)$ and Ω; □: $0.5\cos(0.02\pi t)$ and $0.5\,\Omega$.

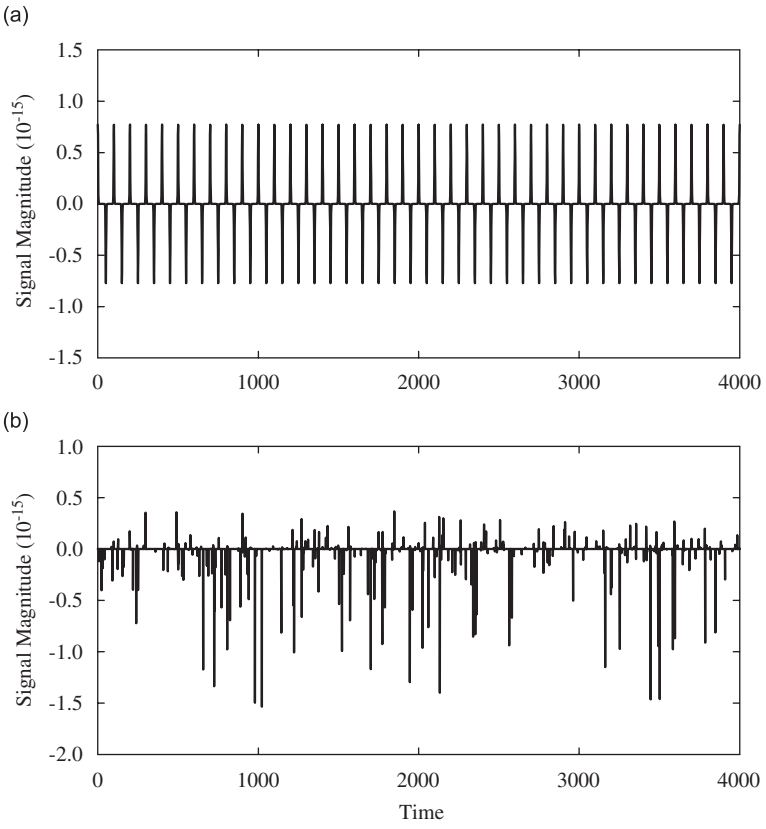

Fig. 5. Time variations of $w^{(4)}$ for $\alpha = \beta = 1$: (a) $0.5\cos(0.02\pi t)$; (b) $0.5\,\Omega$.

3.1. Weak steady sinusoidal signal

The signal in this section consists of a weak sinusoidal signal embedded inside a random background noise and it takes the form of

$$x(t) = 0.5\,\Omega + A\,\sin(0.1\pi t). \tag{6}$$

The S/N is defined as $10\log_{10}(2A)$. Fig. 6 shows the effects of repeated transformations (Eq. (5)) on $x(t)$ for $\alpha=\beta=1$ and $A=0.025$ ($S/N\sim-13$ dB). The spectral power density calculations were done using MATLAB with data segment length of 8192 and 0% overlapping. Figs. 7 and 8 illustrate the corresponding spectral power spectra for $A=0.015$ ($S/N\sim-15$ dB) and 0.007 ($S/N\sim-19$ dB), respectively. The performance of the transformation for $S/N=-20$ dB are very marginal and thus are not presented.

For $A=0.025$, the spectral peak of the sinusoidal wave can be observed even without the transformation, but it is surrounded by the spurious spectral peaks from the noise. It is consistent with the observations made in Section 2. Subsequent transformations make this peak more distinctive from the background (Fig. 6) until $w^{(5)}$. With a weaker sinusoidal wave of $A=0.015$, the spectral peak due to this wave can be recovered distinctively after $w^{(2)}$ as shown in Fig. 7. The performance starts to go worse after the fifth transformation. For $A=0.007$, the spectral peak of the wave can only be recovered satisfactorily after $w^{(4)}$, but again the resolution of this spectral peak becomes poor after $w^{(5)}$. The test is repeated using 100 different random noise samples, but the corresponding results are very similar to those given in Figs. 6–8 and thus are not discussed. The results with larger α or with other values of β do not show any improvement and thus are also not presented. Though the present examples involve signals having a single steady frequency component, the proposed method also works in the presence of multiple steady frequency components (not shown here). The issue of frequency resolution is left to further study.

3.2. Abruptly generated signal that grows exponentially with time

The signal in this section consists of Ω and an exponentially growing sinusoidal wave initiated at time t_i:

$$x(t)=B\Omega+AU(t-t_i)\exp(\gamma(t-t_i))\cos(\omega(t-t_i)), \tag{7}$$

where γ denotes the growth rate of the sinusoidal wave. Without lost of generality, t_i, γ, A and ω are fixed at 1000, 0.002, 0.01 and 0.1π, respectively. The S/N here is defined as $10\log_{10}(A/B)$, which denotes the initial strength of the growing signal relative to the background noise. It is shown in the last section that the proposed transformation can enhance the recovery of a steady and continuous sinusoidal wave in the presence of a background noise down to a S/N of -19 dB. In this section, the main focus is on the recovery of t_i—the instant of wave initiation. The two transformation parameters α and β are fixed at unity.

The moving time frame approach is adopted. The number of data in the time frame is denoted by n. The calculation is commenced by going through the transformations as in the last section using the first n data of $x(t)$. The time frame is then advanced by one time step and the calculations are repeated. Since the performance of the transformations depends on the magnitude of the data series, which can vary widely in practice, the data in each time frame are normalized by the data range (the difference between the maximum and minimum values). The mean value of the data in each time frame is kept to be zero. The number of data put into the Fourier transform calculation is again n, giving a frequency resolution of $1/n$.

Fig. 9 is an example of $x(t)$ with $B=0.5$ such that the $S/N=-17$ dB. Only random background noise exists for $t<0$. One can observe that the sinusoidal wave cannot be seen even at $t=2000$ under this S/N. Fig. 10 illustrates the variation of the maximum spectral power density upon repeated transformations of the signal with $B=0.01$ for $n=200$. Since it is actually unable to know in advance the frequency of the sinusoidal growing signal in reality as far as machine monitoring process is concern, only maximum spectral power density $P_{\max}$ is considered in Fig. 10 and in similar figures presented afterward. The frequency of the sinusoidal wave can be easily found out once it is detected. Certainly, one can anticipate that the maximum power density is equal to that of the growing sinusoidal wave after two transformations. One can notice from Fig. 10 that the spectral power densities of the signals are the smallest near to the instant of the wave initiation. For $n=200$ at this S/N of 0 dB, the minimum $P_{\max}$ appears at $t\sim1010$ after $w^{(3)}$ and a sharp drop in $P_{\max}$ precedes this instant. The largest time gradient of the maximum power density, $|\partial P_{\max}/\partial t|$, appears at $t=1001$ (Fig. 11) which is very close to t_i. Similar results can be obtained when n is reduced to 100, but the analysis fails when n is further halved to 50 (not shown here).

It is found that $|\partial P_{\max}/\partial t|$ is not a very good indicator when the S/N falls below -3 dB (not shown here). Fig. 12 illustrates the effects of S/N on the recovery of t_i using the parameter $|\partial(P_{\max}(x,\omega)/P_{\max}(w^{(3)},\omega))/\partial t|$. One can observe that a sharp rise in the parameter followed by closely packed spurious peaks of significant

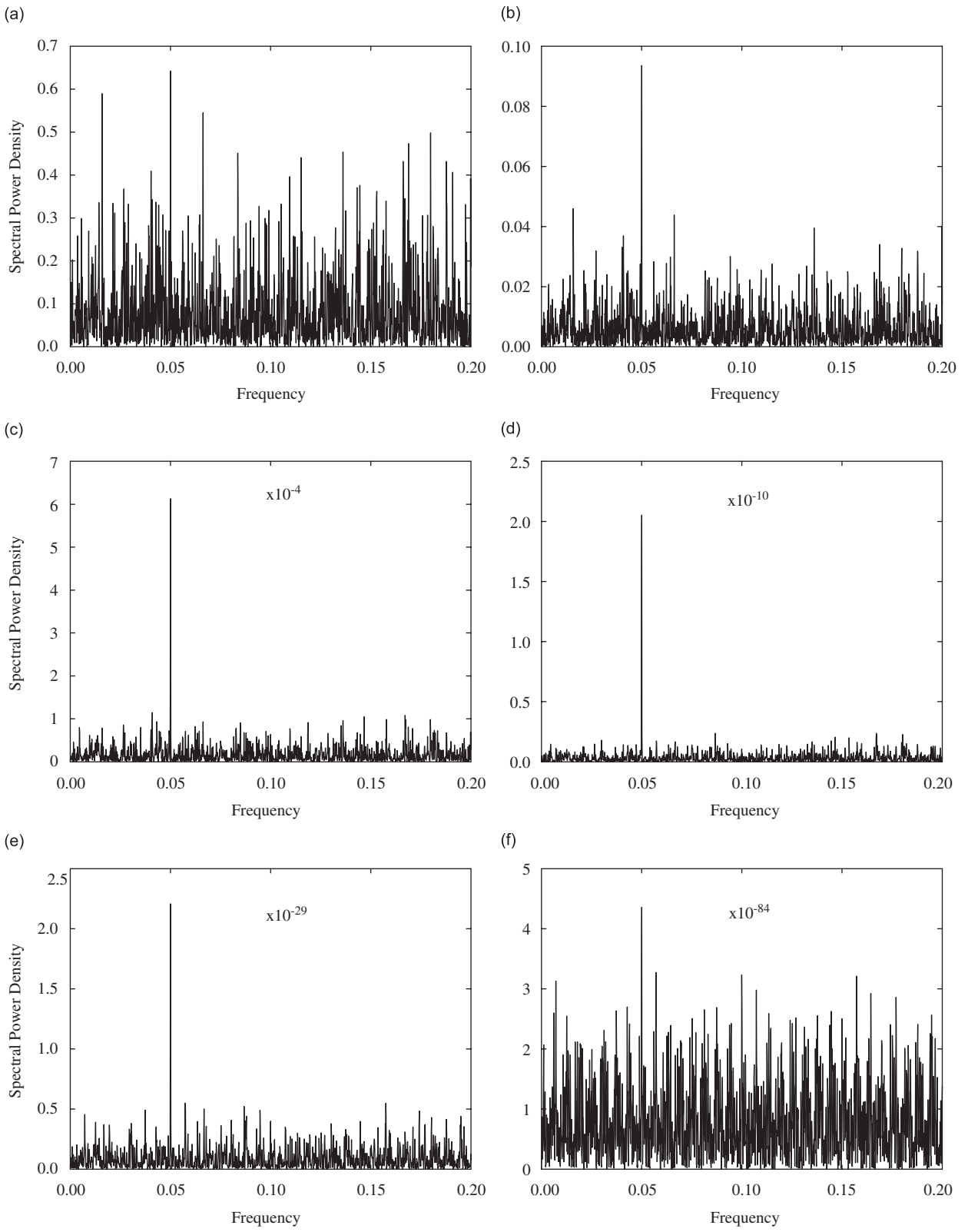

Fig. 6. Effects of repeated transformations on spectral peak recovery in the presence of a background noise Ω for $A = 0.025$ ($S/N = -13$ dB) and $\alpha = \beta = 1$. (a) x; (b) $w^{(1)}$; (c) $w^{(2)}$; (d) $w^{(3)}$; (e) $w^{(4)}$; (f) $w^{(5)}$. Numbers inside the figures denote the multiplication factors for the ordinate axes.

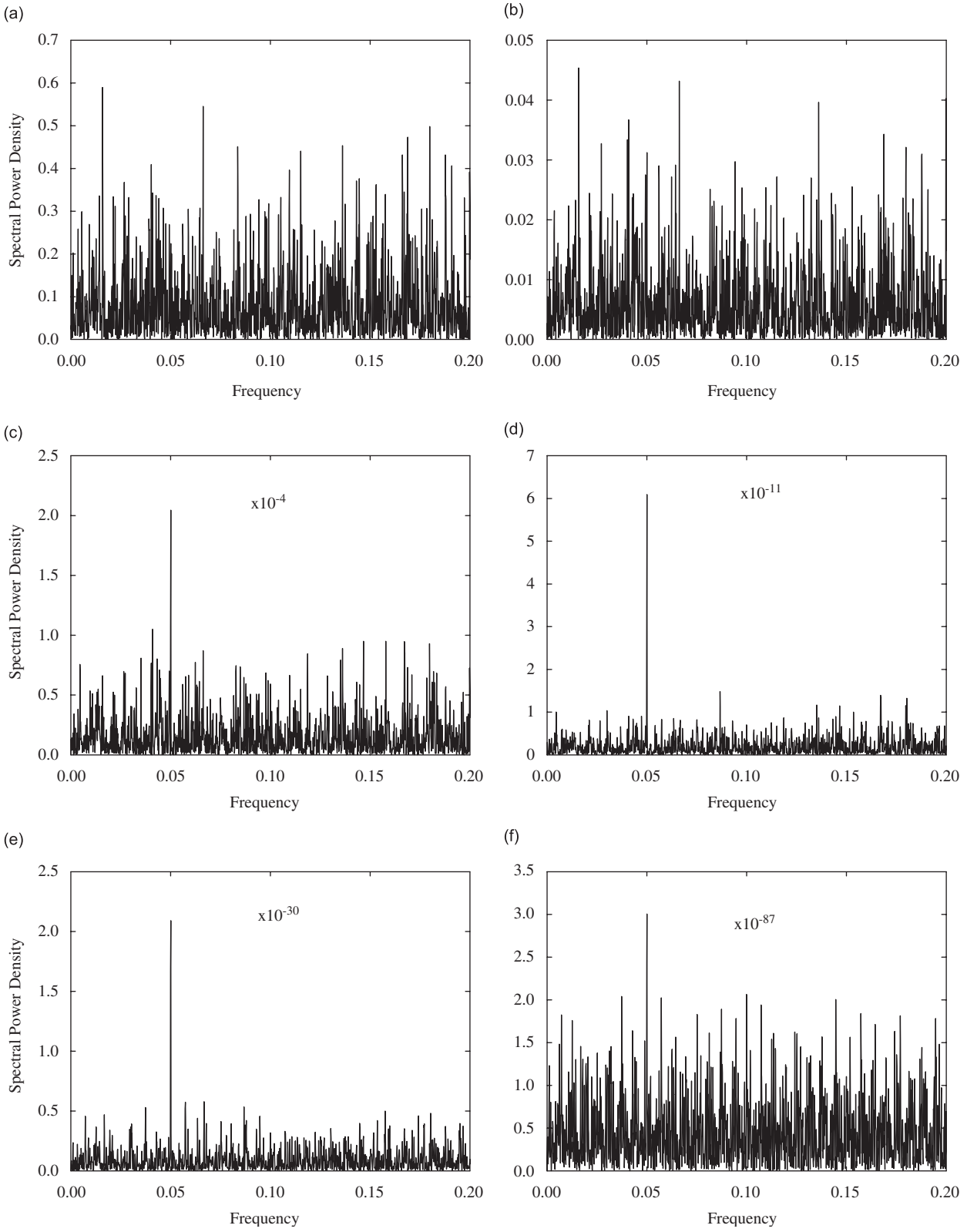

Fig. 7. Effects of repeated transformations on spectral peak recovery in the presence of a background noise Ω for $A = 0.015$ ($S/N = -15$ dB) and $\alpha = \beta = 1$: (a) x; (b) $w^{(1)}$; (c) $w^{(2)}$; (d) $w^{(3)}$; (e) $w^{(4)}$; (f) $w^{(5)}$. Numbers inside the figures denote the multiplication factors for the ordinate axes.

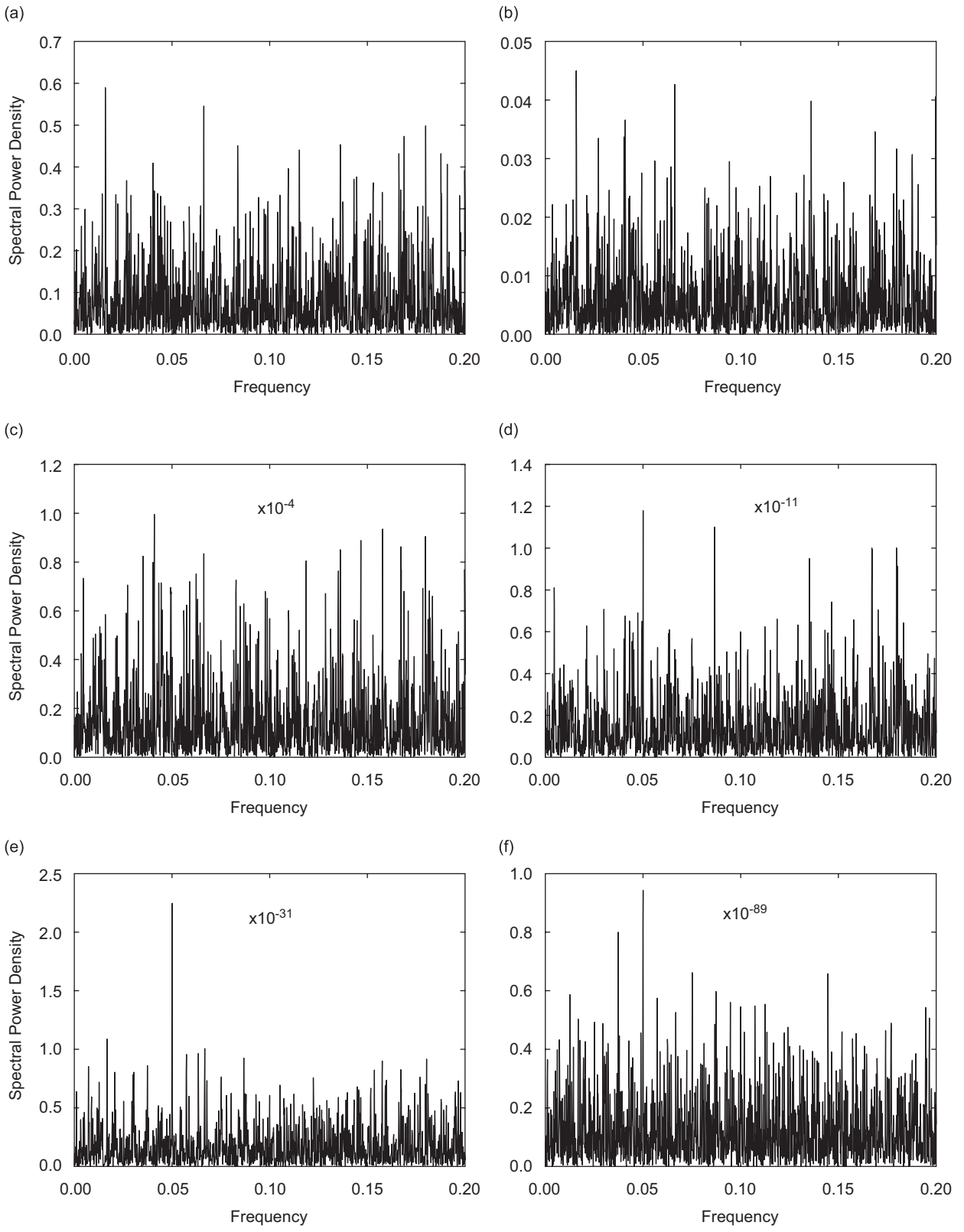

Fig. 8. Effects of repeated transformations on spectral peak recovery in the presence of a background noise Ω for $A = 0.007$ ($S/N = -19$ dB) and $\alpha = \beta = 1$. (a) x; (b) $w^{(1)}$; (c) $w^{(2)}$; (d) $w^{(3)}$; (e) $w^{(4)}$; (f) $w^{(5)}$. Numbers inside the figures denote the multiplication factors for the ordinate axes.

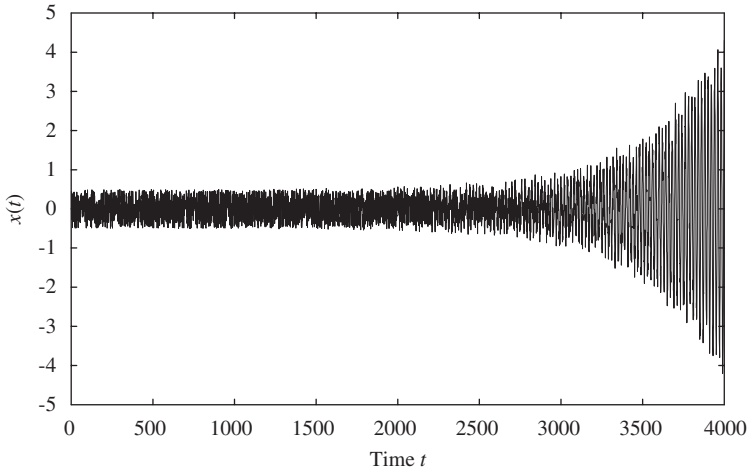

Fig. 9. An example of exponentially growing signal embedded in a background noise. $B = 0.5$ ($S/N = -17\,\mathrm{dB}$).

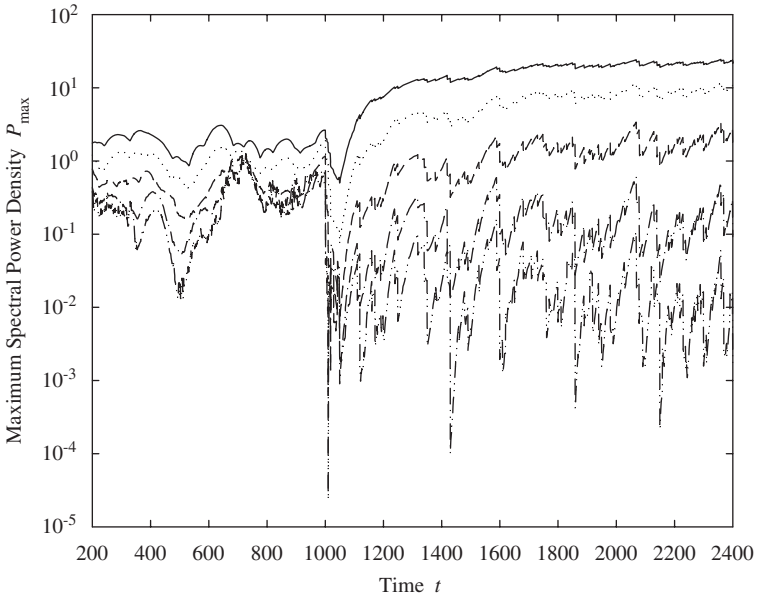

Fig. 10. Time variation of the maximum spectral power density for transformed signals with exponentially growing components. ——: x; ⋯⋯: $w^{(1)}$;— —: $w^{(2)}$;— · —: $w^{(3)}$;— · · —: $w^{(4)}$. $\alpha = \beta = 1$, $n = 200$.

magnitudes can be found at $t \sim t_i$. The recovery of t_i is still satisfactory for a S/N of $-17\,\mathrm{dB}$, although the associated error goes up to ~180 time steps. However, the sinusoidal wave is still not visually distinguishable from $x(t)$ at $t = 300$ (Fig. 9). This parameter also works as good as $|\partial P_{\max}/\partial t|$ for the $S/N = 0\,\mathrm{dB}$ case. It should be noted that the use of $w^{(4)}$ makes the analysis worse and is not discussed. Fig. 12 also indicates that the error of t_i recovery ranges from 0 to a maximum of 230 for a S/N above $-17\,\mathrm{dB}$, but there appears no relationship between the S/N and the magnitude of the recovery error.

The number of data included in the moving average spectral calculation has crucial impacts on the recovery of t_i. It is expected that the increase in n will smooth out spectral irregularities especially within the random background noise and will increase the frequency resolution of the spectral calculation. It is found that a larger n also allows the use of more repeated transformations. The parameter $|\partial(P_{\max}(x,\omega)/P_{\max}(w^{(5)},\omega))/\partial t|$ is

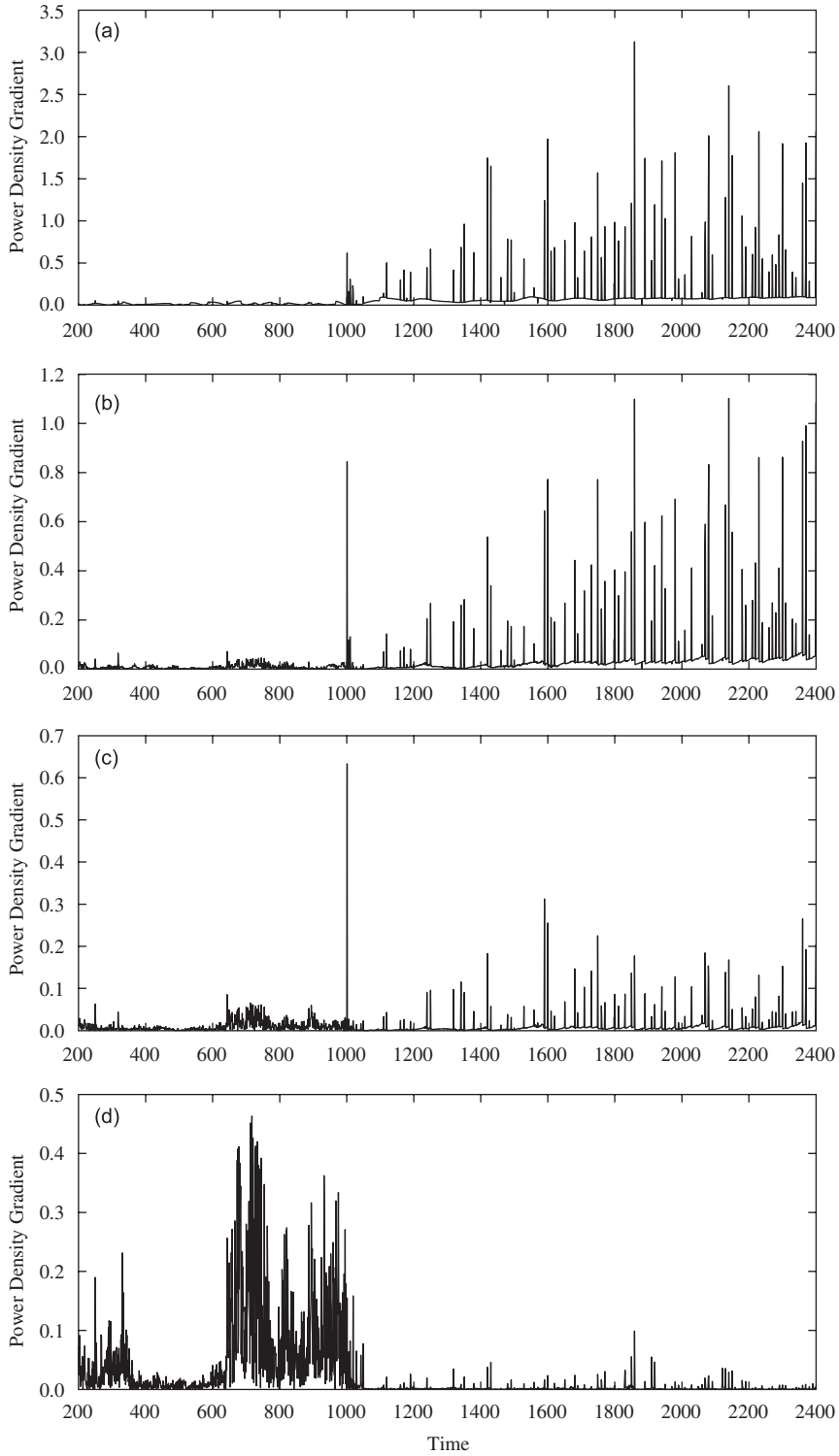

Fig. 11. Time variation of the time gradient of the maximum spectral power density for transformed signals with exponentially growing components: (a) x; (b) $w^{(2)}$; (c) $w^{(3)}$; (d) $w^{(5)}$. $\alpha = \beta = 1$, $n = 200$.

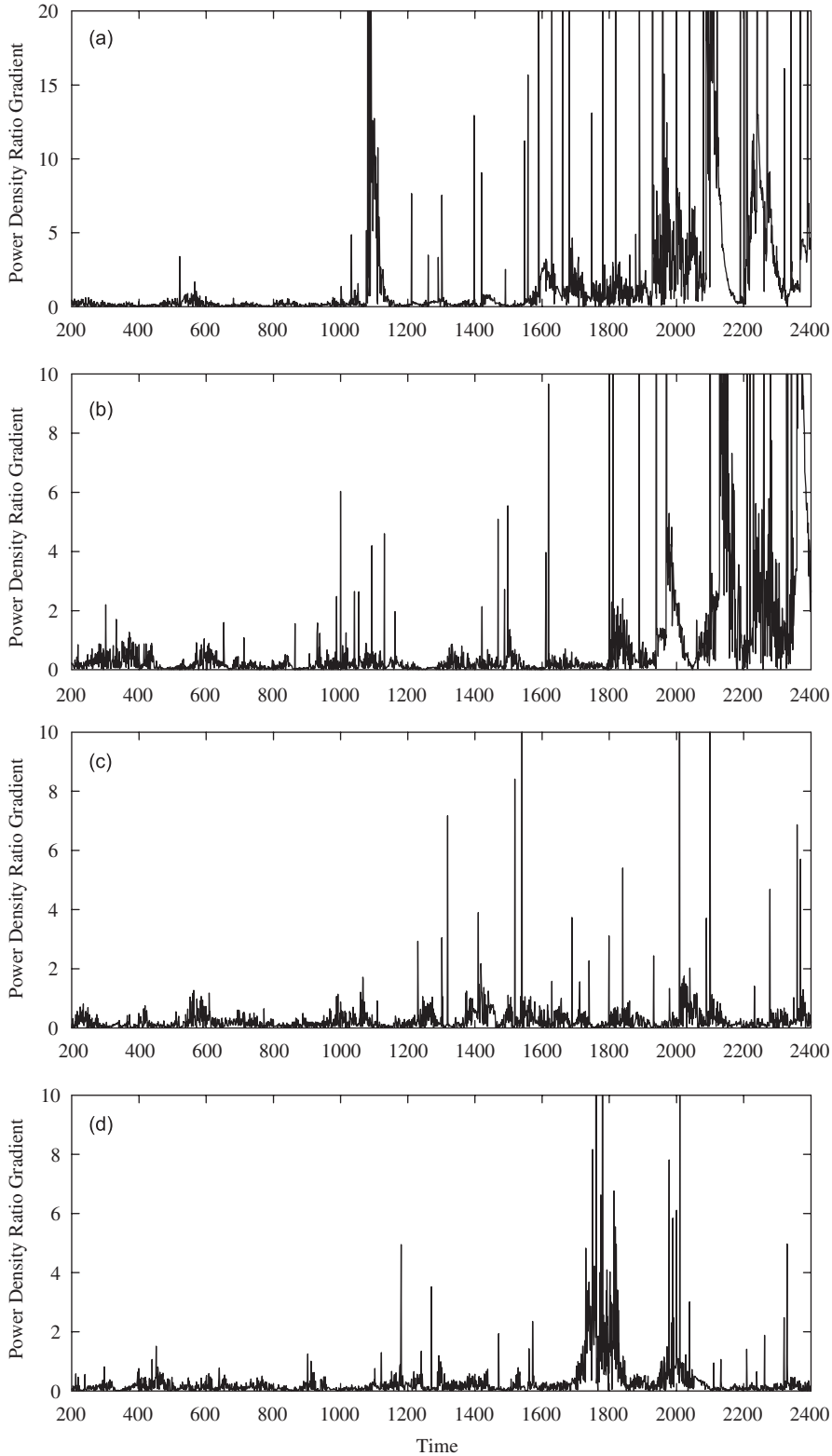

Fig. 12. Time variation of $|\partial(P_{\max}(x,\omega)/P_{\max}(w^{(3)},\omega))/\partial t)|$: (a) $S/N=-7\,\mathrm{dB}$; (b) $S/N=-10\,\mathrm{dB}$; (c) $S/N=-14\,\mathrm{dB}$; (d) $S/N=-17\,\mathrm{dB}$. $\alpha=\beta=1$, $n=200$.

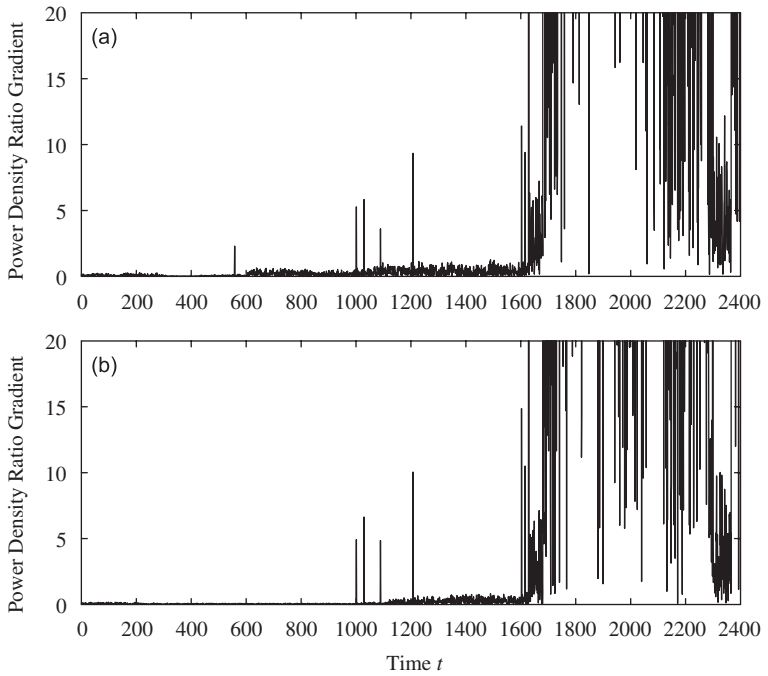

Fig. 13. Effect of n on the recovery of t_i using $|\partial(P_{\max}(x,\omega)/P_{\max}(w^{(5)},\omega))/\partial t|$: (a) $n = 4000$; (b) $n = 8000$. $\alpha = \beta = 1$, $S/N = -17$ dB.

adopted in Fig. 13, where the associated S/N equals -17 dB. One can observe from Fig. 13a that the associated error in the recovery is negligible for $n = 4000$, though there is a small spike at $t \sim 550$ due to the random background noise. The recovery is unambiguous when n is increased to 8000 (Fig. 13b).

It should be noted that the present method may not produce good results in the presence of multiple unsteady frequency components if their frequencies are not known in advance and they are initiated at different instants, unless the STFT is applied. However in many building services applications, the problematic frequencies are usually known in advance [4] and thus the present method can be readily applied with the use of the appropriate numerical/digital filter settings.

4. Conclusions

A novel but simple method for the detection of weak signals embedded in a non-stationary strong broadband background noise is derived in the present study. A function, which tends to transform sinusoidal wave into a regular pulse train, is proposed to be used together with the Fourier transformation. Its performance is illustrated using two artificial numerical examples. The first one is a very weak but steady sinusoidal signal, while the other an exponentially growing sinusoidal wave generated abruptly within the background noise. For the latter, the recovery of the instant of wave initiation is the focus. The performance of repeated transformations on the signals is also investigated.

For the steady sinusoidal wave, the proposed transformation function enables its unambiguous detection even when the S/N drops to -19 dB after the fourth transformation. Further transformation is found to make thing worse and is not recommended. The recovery of the instant of the exponentially growing wave initiation is also enhanced after the application of the transformation function. The associated error is found to be within 300 time steps even for an initial S/N of -17 dB when 200 data are used in the spectral calculation. The recovery of the instant of the wave initiation is improved remarkably by increasing the number of data involved in the calculation. The recovery error becomes negligible when more than 4000 data are used to produce the moving spectral averages.

Acknowledgments

CMC is supported by a staff development scheme of the Hong Kong Community College, The Hong Kong Polytechnic University.

References

[1] W.L. Stutzman, G.A. Thiele, *Antenna Theory and Design*, Wiley, New York, 1998.
[2] Y. Gao, M.J. Brennan, P.F. Joseph, A comparison of time delay estimators for the detection of leak noise signals in plastic water distribution pipes, *Journal of Sound and Vibration* 292 (2006) 552–570.
[3] J. Armstrong, *Condition Monitoring—An Introduction to Its Application in Building Services*, TN 1/86, BSRIA, 1986.
[4] R.B. Randall, *Frequency Analysis*, Brüel & Kjær, Nærum, Denmark, 1987.
[5] C.H. Hodges, J. Power, J. Woodhouse, The use of the sonogram in structural acoustics and an application to the vibrations of cylindrical shells, *Journal of Sound and Vibration* 101 (1985) 203–218.
[6] T.J. Wahl, J.S. Bolton, The application of the Wigner distribution to the identification of structure-borne noise components, *Journal of Sound and Vibration* 163 (1993) 101–122.
[7] B. Basu, V.K. Gupta, Wavelet-based analysis of the non-stationary response of a slipping foundation, *Journal of Sound and Vibration* 222 (1999) 547–563.
[8] S.K. Tang, On the time–frequency analysis of signals that decay exponentially with time, *Journal of Sound and Vibration* 234 (2000) 241–258.
[9] D.E. Newland, Harmonic and musical wavelets, *Proceedings of the Royal Society of London, Series A*, Vol. 444, 1994, pp. 605–620.
[10] Y.M. Zhan, A.K.S. Jardine, Adaptive autoregressive modeling of non-stationary vibration signals under distinct gear states—part 2: experimental analysis, *Journal of Sound and Vibration* 286 (2005) 451–476.
[11] C.M. Chan, S.K. Tang, H. Wong, On analysis of exponential decaying pulse signals using stochastic volatility model, *Journal of the Acoustical Society of America* 119 (2006) 1519–1526.
[12] C. Li, L. Qu, Application of chaotic oscillator in machinery fault diagnosis, *Mechanical Systems and Signal Processing* 21 (2007) 257–269.
[13] J.S. Bendat, A.G. Piersol, *Random Data: Analysis and Measurement Procedures*, Wiley, New York, 1986.